Evolution of $sd - fp$ shell gap for upper sd shell nuclei

M. Saha Sarkar[1]*
[1] *Saha Institute of Nuclear Physics, Kolkata 700064, INDIA*

The intruder orbitals from the fp shell play an important role in the structure of nuclei around the line of stability in the upper sd shell. We have studied ^{35}Cl, ^{30}P, ^{36}Cl, ^{37}Ar and ^{35}Ar experimentally using the INGA setup. Large basis cross-shell shell model calculations have indicated the need for change of the $sd - fp$ energy gap for reliable reproduction of negative parity and high spin positive parity states. From this observation along with those of other groups, the $sd - fp$ shell gap appears to evolve as a function of proton number. The role of reduction of pairing in the erosion of shell gaps in neutron rich nuclei in this mass region as well in other regions have been investigated using empirical data. A simplistic CHFB calculation using pairing plus quadrupole Hamiltonian has also been done to understand the feature theoretically.

1. Introduction

The sd shell nuclei in the neighbourhood of doubly closed ^{40}Ca are suitable for applications of spherical shell model calculations. The untruncated calculations in the sd valence space have been fairly successful in reproducing spectroscopic data pertaining to the ground states and the low lying positive parity states of several nuclei of this mass region close to the stability line. However, for negative parity states and higher spin positive parity ones, intruder configurations from the neighbouring fp shell become relevant. The need for changes of the $sd - fp$ energy gap for reliable reproduction of negative parity and high spin positive parity states of upper sd shell nuclei have been pointed out by several workers [1–3]. Apart from the spherical single particle excitations, the spectroscopy of several nuclei in the mass region revealed deformed states (even superdeformation) at low-excitation energies, indicating that the nuclei near the closed shell with Z or N = 20 can easily lose spherical shape [4, 5]. Large-scale shell model calculations to interpret superdeformed band in ^{36}Ar[4] have provided a microscopic description of rotational motion in nuclei.

Spectroscopy of the nuclei in this mass region has been studied since 1960s. But till late 80s, due to the experimental limitations, mostly low spin states were reported. In the recent years, utilising the sophisticated techniques of gamma spectroscopy, high spin states of several nuclei in this mass region have been observed. The issue of violation of mirror symmetry and the vanishing N = 20 shell gap in neutron rich nuclei have also evoked immense interest among the community.

The gamma spectroscopic studies of these light mass nuclei are very much different from those of the heavier ones. The light nuclei have lower Coulomb barriers, so the number of competing channels with evaporation of charge particles becomes very large with increasing excitation energy of the compound nucleus. As in most of the cases the structure of these nuclei are dominated by shell model states, these are low multiplicity experiments. The valence space of the nucleons does not contain high spin orbitals (highest spin orbital is $1f_{7/2}$). So the angular momentum of the compound system is also restricted. The light masses of the reaction products in the fusion reaction also result in lower angular momentum. The transition energies are usually very high ($\simeq$ 2-3 MeV) where the efficiencies of the normal HPGe detectors fall off very sharply. As the spin increases, the energies of the transitions become higher implying lower detection efficiency and poorer resolution. In this respect the Clover detectors in their addback mode show excellent improvement over the normal detectors [6]. So our Indian Na-

*Electronic address: maitrayee.sahasarkar@saha.ac.in

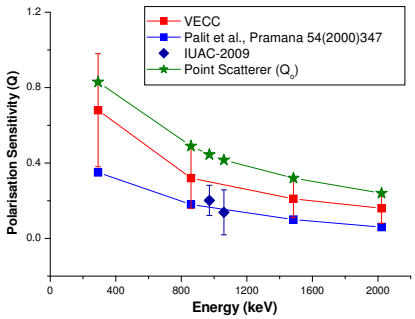

FIG. 1: The polarisation sensitivity of a Clover detector in different implementations of INGA. See text for detail.

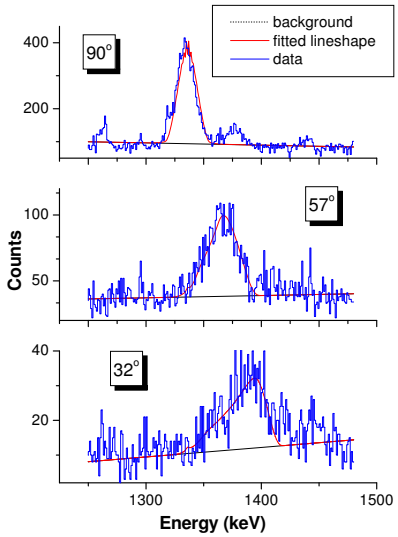

FIG. 2: One of the totally shifted gammas of ^{35}Cl observed at different angles.

tional Gamma Array (INGA) [7] comprising of Clover detectors is an ideal setup for studying this mass region. The high velocities of the recoiling light nuclei and the effect of evaporation of charged particles (like α particles) on the kinematics increase the width of the gamma peaks considerably. In that way also, composite detectors like Clovers help corrections for Doppler broadening and shifts.

This work was initiated through the gamma spectroscopic studies of fusion evaporation reaction residues at our various accelerator facilities using our INGA ([7]) comprising of CLOVER detectors. The present work will encompass a few observations and related queries which we experienced while studying nuclei with A<40 lying on or close to the line of stability. Eventually we found that these queries may also have relevance for the studies of neutron rich nuclei in this mass region as well as those near doubly closed ^{132}Sn away from stability.

2. Experimental details

In most of our experiments at different accelerator centres we have used reactions in inverse kinematics. Use of inverse kinematics resulted in large velocities of the recoils (β= v/c = 5-6%), confined to a narrow cone (half angle 13^o) in the forward direction facilitating observation of large lineshape. The same reaction in the forward kinematics would lead to recoil velocity of 2.5% of c, moving in a cone with a half angle of $\simeq 31^o$. The spread in the recoil velocities is within 7% in the inverse reaction compared to 17% in forward reaction. This reduction in the spread of recoil velocity is useful in decreasing the uncertainty in the fitting of the lineshapes. But the large shifts and broadening also pose additional problems in some cases.

A. Study of ^{35}Cl

The work is based on data from earlier implementations of INGA setup comprising of eight Compton suppressed Clover detectors. The first experiment was performed at Tata Institute of Fundamental Research (TIFR), Mumbai, using 70 MeV ^{28}Si beam from 14UD BARC-TIFR Pelletron. The second experiment was performed at Inter-University Accelerator Centre (IUAC, formerly, known as Nuclear Science Centre (NSC)), New Delhi, using 88 MeV ^{28}Si beam from 15UD Pelletron. Both the experiments employed the ^{12}C(^{28}Si,αp) ^{35}Cl fusion-evaporation reaction. The target was $\simeq 50\mu$g/cm^2 carbon backed by 10.5 mg/cm^2 gold. The details about the experimental setup may obtained from ref. [1].

B. Study of ^{30}P

The experiment was performed at the TIFR, Mumbai. This was also done using earlier implementation of INGA with eight Compton suppressed Clover detectors. The detectors were arranged in the horizontal plane. The setup is discussed in Ref. [2]. The setup had a solid angle coverage of $\simeq$6% of 4π. The full energy peak efficiency of the array at 1 MeV was 1.3%. A 500 μg/cm^2 ^{24}Mg target with thick Ni backing (sufficient to stop the recoils) was bombarded with the 40 MeV ^{16}O. A thin layer of oxide (containing ^{nat}O) was present on the surface of the target. The natural abundance of ^{16}O amounts to 99.8%. The nucleus ^{30}P was populated in the $^{16}O(^{16}O, pn)$ reaction.

C. Study of ^{37}Ar, ^{36}Cl

150 μg/cm^2 thick ^{27}Al target with 15.4 mg/cm^2 thick gold backing (sufficient to stop the recoils) was bombarded with 66 MeV ^{14}N beam provided by the BARC-TIFR Pelletron, Mumbai. The details about the experimental setup may be obtained from ref. [8]. Excited states of ^{37}Ar were populated in this experiment. Excited states of ^{36}Cl were populated in another experiment where 9.9 mg/cm^2 thick ^{27}Al target was bombarded by 115 MeV ^{16}O beam at Variable Energy Cyclotron Centre, Kolkata. This experiment was done during the Kolkata campaign of INGA setup. The other details about the experimental setup may be obtained from ref. [8].

D. Study of ^{35}Ar, ^{35}Cl

High-spin states in ^{35}Cl and ^{35}Ar have been populated through $^{12}C + ^{28}Si$ (110 MeV) reaction in the inverse kinematics. The target was ^{12}C (50 μg/cm^2) evaporated on $\simeq$18 mg/cm^2 gold backing. Gamma - gamma coincidence measurement has been done using thirteen Compton suppressed Clover detectors (INGA setup) at Inter University Accelerator Centre (IUAC), New Delhi. In the set up, the power supplies, INGA modules, 8 channel 13 bit CAMAC ADC-814 and the Multi CAMAC Crate data acquisition system CANDLE [9] were all developed at IUAC. The other details about the experimental setup may be obtained from ref. [10].

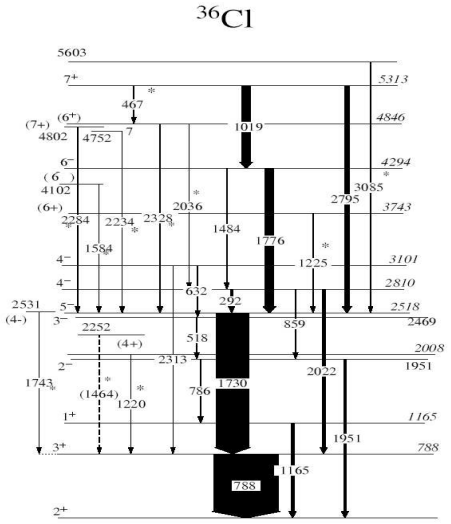

FIG. 3: Partial level scheme for ^{36}Cl observed in the present work. The new gammas found are marked by asterisk.

3. Experimental Analysis

In most of the cases, the analysis program INGASORT [11] was used for sorting the raw data into matrices and for generation of background subtracted gates from these matrices. Many of the gamma rays depopulating the excited states in the nuclei in this mass region have very high energies ($\simeq$ 2000 keV or more). Since suitable radioactive sources having gamma rays of energies greater than 1500 keV are not easily available, the energy and efficiency calibration of the Clover detectors were done using sources of ^{60}Co, ^{152}Eu and ^{66}Ga ($T_{1/2}$ = 9.41 h). The ^{66}Ga source having gamma-rays from 833 to 4806 keV was prepared through $^{52}Cr(^{16}O,pn)^{66}Ga$ reaction at 55 MeV [6].

In these experiments, because of the opening up of a large number of reaction channels and presence of many overlapping γ -rays, the relative intensities have been extracted from γ - γ symmetric matrices having data from all the detectors on both the axes. The multi-

polarities of γ transitions have been obtained through a measurement of directional correlation of γ -rays deexciting oriented states or DCO ratios from the coincidence data by using the detectors placed at specific convenient angles depending up on the particular detector setup. For assignment of spins and γ -ray multipole mixing ratios δ, the experimental DCO ratios were compared with the theoretical ones using the program ANGCOR [12]. In all the experiments, the Clover detectors were used as polarimeters for measuring polarization of gamma-rays to determine the electric or magnetic character of transitions. The sensitivity of different implementations of INGA setup are shown in Fig.1. The IUAC-2009 and the earlier measurements of Palit *et al.* [13] agree. The VECC setup showed some what better sensitivity. The sensitivity for an ideal point scatterer is also shown in the figure for comparison. We have performed integrated polarization asymmetry measurements (IPDCO) [1]. For this purpose two asymmetric IPDCO matrices named parallel and perpendicular were constructed from the data. The parallel matrix was constructed having on first axis the simultaneous events recorded in the two crystals (of the 90^o Clover detector) which were parallel to the emission plane and on the second axis the coincident gamma rays registered in any other detector. Similarly, the perpendicular matrix consisted of simultaneous events recorded in the two crystals which were perpendicular to the emission plane on first axis and the second axis consisted of the coincident gamma rays from any other detector. The details about our analysis may be found in any one of our previous work [1, 2, 8, 10].

Lifetime analysis using Doppler Shift Attenuation Method (DSAM) was done using asymmetric γ γ coincidence matrices having on one axis events from the detector at a particular angle and on the second axis the coincident gamma rays registered in any other detector. Level lifetimes were extracted using both the centroid shift method and the lineshape analysis [1]. Lineshape analysis of the Doppler shifted spectra was done using the code LINESHAPE [14] which simulated the slowing down history of the recoils in the target and the backing, using Monte Carlo technique. The details of the lineshape fitting is discussed in Ref. [1].

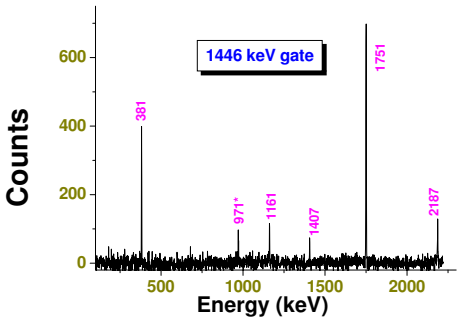

FIG. 4: A representative gated spectrum for ^{35}Ar observed in the our work .

4. Experimental Results

A. ^{35}Cl

^{35}Cl is a stable nucleus in this mass region. The primary objective of this work was to investigate high-spin states of this nucleus and characterise them by measuring their spin-parities and lifetimes. The partial level scheme of ^{35}Cl, has been established [1] using the coincidence relationship, relative intensities, RDCO and IPDCO ratios of γ -rays. The level scheme has been extended up to $\simeq$ 11 MeV. Gamma transitions energies along with their relative intensities and RDCO values from data of both the experiments and the polarization asymmetry (IPDCO) values different γ -rays are extracted. Seven levels have been placed in the level scheme [1]. Estimation of lifetimes and limits for them have been provided for a number of levels. Gamma transitions from some the levels were totally shifted in the spectra generated from IUAC data. None of them showed any stopped component. This feature indicated that all these gamma rays were emitted in flight. The carbon target used in the present experiment was very thin, where energy losses of the recoils

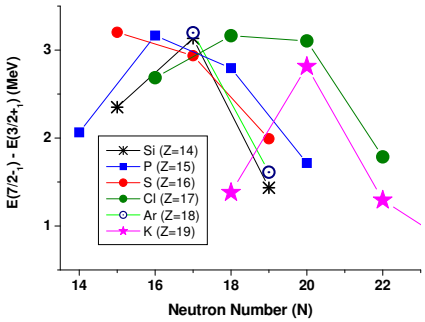

FIG. 5: The energy differences between the first $7/2^-$ state with first $3/2^+$ states as a function of neutron number.

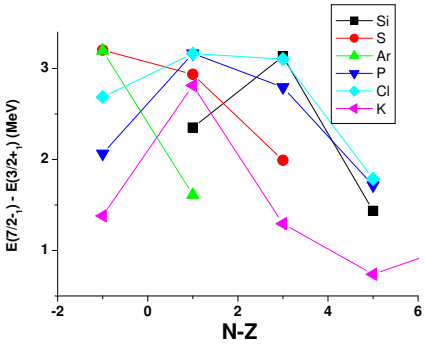

FIG. 6: The energy differences between the first $7/2^-$ state with first $3/2^+$ states as a function of (N-Z).

were negligibly small. The backing was of thick gold. So we concluded that these levels definitely have effective lifetimes shorter than the stopping time of the recoils in the backing material. Moreover, even the contributions in lifetimes from side feedings must be very small. It also indicated that these gamma rays were emitted from excited levels at high energies.

B. ^{30}P

The self-conjugate nucleus ^{30}P having seven valence protons and the same number of neutrons with respect to the ^{16}O inert core is in the middle of the *sd* shell. For ^{30}P, the number of low-lying configurations which can mix is expected to be sufficient to make highly configuration mixed states more probable. So the onset of collectivity might be expected in it and it is interesting to study the evolution of collectivity manifested in terms of large configuration mixing. The partial level scheme of ^{30}P, has been established [2] using the coincidence relationship, relative intensities, RDCO and IPDCO ratios of γ -rays. The branching ratios are also determined and tabulated in Ref. [2]. The first polarisation measurement for this nucleus has been done in this work. The spin-parity assignments of a few levels up to about 7 MeV has been confirmed. We concluded that more heavy ion data at higher excitation energies are needed to study the extent of collectivity developed at higher spins.

C. ^{37}Ar, ^{36}Cl

For these nuclei also, the primary objective of the experimental investigation was to study and characterise their high-spin states by measuring their spin-parities and lifetimes. Data analysis has been completed. For both the isotopes, a few new levels have been included in the scheme. Fig.3 shows the level scheme for ^{36}Cl. Lifetimes have also been measured. Polarisation data have been analysed to assign and confirm spin and parities of the observed levels.

D. Study of ^{35}Ar, ^{35}Cl

Mirror nuclei are a pair of nuclei where the number of protons and neutrons are interchanged. The study of differences between excitation energies of analogue states in mirror pairs (Mirror Energy differences or MED) has been pursued to test the charge symmetry of nuclear force. A complementary way to test isospin symmetry is based on investigation of the electromagnetic decay properties in mirror pairs. Anomalous MED in *sd* shell nuclei, ^{35}Ar and ^{35}Cl has been observed [15]. So far the electromagnetic decay properties deduced from the level lifetimes in this mirror pair have not been compared. In this work, we have done measurements of lifetimes of excited

higher spin levels of ^{35}Cl and determined mixing ratios of a few gamma transitions in ^{35}Ar. Polarisation asymmetry of some gamma rays of ^{35}Cl and a few of ^{35}Ar have been determined. These data along with the assumption of isospin symmetry will provide estimate of lifetime of important levels in ^{35}Ar necessary for planning future experiments.

5. Discussions

A. Salient features in the excitation spectrum of ^{35}Cl and Shell Model studies

The ^{35}Cl nucleus with Z=17 and N=18 has nine (9) valence protons and ten (10) valence neutrons beyond ^{16}O core. From our data, we find the lowest positive parity state at 1763 keV and the most intense gamma ray in ^{35}Cl is emitted from the lowest negative parity state at 3163 keV. For shell model calculations, merely considering the *sd* shell is not enough. Inclusion of a negative parity orbital in the valence space is essential to explain even the low energy spectrum. In particular for the negative parity states (even for the positive parity states of relatively higher spins), one needs a nuclear Hamiltonian over the $sd-fp$ valence space. The details of shell model calculations have been discussed in Ref. [1].

The Hamiltonian ($sdpfmw$) used (Ref. [1] and references therein) thus consists of three parts, viz., $sd-$ and $fp-$ shell interactions and the cross-shell ones. It consists of Wildenthals matrix elements for the *sd* shell, Mcgrory's Hamiltonian for fp shell and modification of the Millner-Kurath interaction for the cross-shell components. For the positive parity states, $0\hbar\omega$ excitation has been considered, i.e only the full *sd* shell has been used as the valence space. Low energy positive parity spectra are reproduced quite accurately [1]. But the energies for higher spin positive parity states beyond $9/2_1^+$ are predicted substantially higher than the experimental ones indicating the insufficiency of the valence space. The nucleon excitations to the neighbouring fp shell are therefore essential even for high spin positive parity states.

For the negative parity states, simplest way to get them is through $1\hbar\omega$ excitation, i.e. only 1p1h, *sd* to fp excitations are allowed. It is observed that the calculated energies of the negative parity levels are consistently higher compared to the experimental values. This was also observed by previous workers (Ref. [1] and references therein), where the predictions for negative parity states with accuracy better than 500-600 keV were found to be difficult. This was attributed to the overestimation of the $sd-fp$ gap in the corresponding interaction. To improve the agreement for the negative parity states and high spin positive parities, we have depressed the single particle energies (SPES) of $1f_{7/2}$ and $2p_{3/2}$ so that the first negative party state is reproduced.

Dramatic improvement of results was observed. We found that excitations to fp shell are essential to reproduce even the positive parity higher spin states. The $sd-fp$ shell gap has to be decreased to reproduce both positive and negative parity energy levels. We have similar observations for ^{30}P [2], ^{36}Cl and ^{37}Ar [8].

But recently, in a study [3] of the high-spin structure of ^{37}Cl, M. Ionescu-Bujor *et al.* indicated that the shell gap between the *sd* and fp shells produced by the interaction ($sdfp$) used by them was somewhat underestimated and they felt a need for increasing the $sd-fp$ gap to reproduce their data. On the other hand, when they used another interaction $SDPF-M$, this gap was overestimated and there was a need for decreasing the $sd-fp$ gap.

B. The choices of single-particle energies and the $sd-fp$ shell gap

So these observations along with those of ours indicated that the issue of $sd-fp$ shell gap needs more careful investigation. The single-particle energies (SET A) are used in interactions like $SDPF-M$, $sdpfmw$, etc. to reproduce the neutron separation energies and the one particle spectra of ^{17}O (sd shell) and ^{41}Ca (fp shell). These interactions over predict energies of negative parity states indicating that the $1d_{3/2}-1f_{7/2}$ gap produced may be too large. So for this set A, reduction of spes of fp orbitals improves results for high spin positive parity and low spin negative

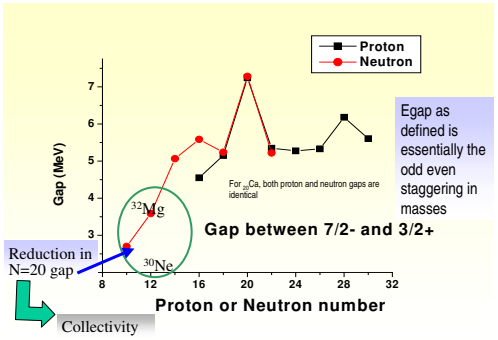

FIG. 7: Evolution of energy gaps E_{gap} for Z=20 (N=20) as a function of neutron(proton) numbers.

parity states dramatically.

But the *sdfp* effective interaction used in Ref. [3] takes ^{28}Si as a core, and the single-particle energies (SET B) are chosen in order to reproduce the single-particle states in ^{29}Si. In this case the calculated energies are systematically smaller than the experimental energies indicating that the shell gap between the *sd* and *fp* shells produced by the *sdfp* interaction is somewhat underestimated. So to reproduce the data there is a need for increasing the $1f_{7/2}$ and $2p_{3/2}$ single-particle energies.

If the intruder spes are estimated from ^{41}Ca spectra with respect to ^{16}O core, this gap needs to be reduced for reproduction of ^{30}P, $^{35,36}Cl$ and ^{37}Ar spectra. The difference in binding energy between ^{41}Ca and $^{40}Ca = 8.36$ MeV gives the s.p. energy of $1f_{7/2}$ state w.r.to ^{40}Ca as the inert core. On the other hand, if one takes ^{28}Si as a core and chooses the spes in order to reproduce the single-particle states in ^{29}Si, it is found that the $sd-fp$ gap comes to be around 2.5 MeV, thus needs a small increase to reproduce the experimental data for ^{37}Cl. In this way, the $sd-fp$ shell gap appears to evolve as a function of proton number.

An alternative solution to changing the spes could be to change the matrix elements of the effective interaction that connect the *sd* with the *fp* shell. But this needs a dedicated theoretical work involving enough experimental information about negative parity as well as high spin positive parity states of these nuclei. Usually the single-particle energies (spes) used in these Hamiltonians are devoid of the influence of the cross-shell interactions and have to be re-adjusted to reproduce the observed energy spectra. Computational limitations due to large dimensionality problem lead to the truncation of the model space. This may also require an readjustment of the spes. This may have direct relevance to the island inversion observed for neutron rich isotopes in this mass region. In Fig. 5. the energy differences between the first $7/2^-$ state with first $3/2^+$ states for odd A nuclei in this mass region ranging from Si (Z=14) to K(Z=19) have been plotted to follow empirically the change of the $sd-fp$ shell gap. Due to lack of information regarding the spectroscopic factors of these states, the y axis shows energy values of the lowest energy states with angular momentum j and not those with the quantum numbers (nlj) of the single-particle orbits, *viz.*, $1d_{3/2}$ and $1f_{7/2}$. As the shell model calculations are usually performed in the JT formalism, the plot also does not distinguish whether the state arises from a neutron or proton orbital. In Fig. 6, the same energy differences are plotted as function of (N-Z) according to the suggestion of Ref. [16], where the authors proposed that the position of the intruder state is dependent almost entirely on N-Z. Both the Figs. 5 and 6 show no regular variation of this energy gap with N and N-Z. But it is clear that for $^{35-37}Cl$, the energy difference is $\simeq 3-3.2$ MeV, which is larger than that for ^{29}Si ($\simeq 2.2$ MeV), But definitely smaller than that in ^{41}Ca ($\simeq 8$ MeV).

C. Evolution of gaps

We have already shown from the experimental data that the spherical N = 20 gap is relatively small to allow excitations in the *fp* shells. As *fp* orbits lie outside the normal model space of the *sd* shells, they are often referred to as intruder states. For some nuclei, the intruder and normal configurations are inverted in energy. They belong to the so-called "Island of Inversion" [17, 18]. Evolution of energy gaps $E_{gap}(Z_{magic}, \mathrm{N})$ or $E_{gap}(Z, N_{magic})$ formed between occupied and valence proton

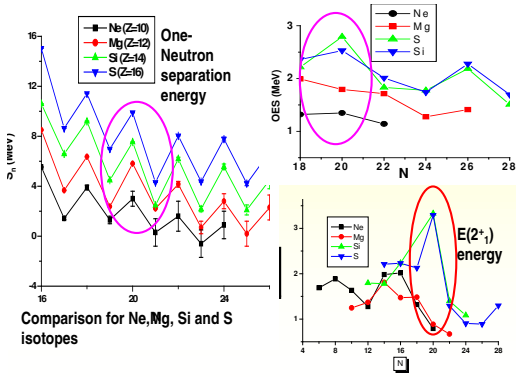

FIG. 8: Correlation of S_n, OES and E(2_1^+) for Ne, Mg, Si and S isotopes.

or neutron single particle orbitals have been studied by Sorlin and Porquet [17]. They suggested a methodology, which has to be limited to spherical nuclei. They have also pointed out that while determining the energy gap, the mean-field potential, which is an average of nucleon - nucleon interactions inside a nucleus, may change slightly between the nuclei with Z_{magic} and Z_{magic} + 1 which are used in the relation to define the size of the gap, $E_{gap}(Z_{magic}$, N). Therefore, the intrinsic value of $E_{gap}(Z_{magic})$ determined by that relation will be approximate. But if one wants to track the evolution of the gap along an isotopic chain, it may provide new information on the modification of shell closures. The relations to determine these gaps are given by [17]: $E_{gap}(Z_{magic}, N) = S_p(Z_{magic}, N) - S_p(Z_{magic} + 1, N)$ and $Egap(Z, N_{magic}) = S_n(Z, N_{magic}) - S_n(Z, N_{magic} + 1)$. The Fig. 7 shows the variation of the shell gaps at N = 20 or Z=20 with proton or neutron numbers. In Ref. [17], the neutron N=20 gap is not shown for Z < 14, as the size of the N = 20 spherical gap can no longer be obtained due to the onset of deformation at those isotopes. The $3/2^+$ ($7/2^-$) states in them therefore will not carry the information about the $1d_{3/2}$ and $1f_{7/2}$ states only.

In the present work, in Fig.7, we have shown the so called "gap" till Z=10. Reduction in this N=20 energy gaps for the isotopes where collectivity is known to set in should be noted. Now let us look back once again to the definition of the $E_{gap}(Z, N_{magic})$ given in Ref. [17]. It essentially represents the odd even staggering (OES) in masses.

D. Odd-even Mass Staggering (OES)

Odd-even mass staggering has generally been associated with the pairing gap, as suggested by BCS theory. Several mechanisms contribute to OES in the framework of the mean-field theory. They contain information [19] on, (i) single-particle energies, (ii) BCS pairing, and (iii) orbital interaction energies. One defines [19] the neutron OES as

$$\Delta_n^{(3)}(N, Z) = -(-)^{\pi_N}\frac{1}{2}(S_n(N+1, Z) - S_n(N, Z)) \quad (1)$$

Here S_n is the one neutron separation energy, $S_n(N)$ = B(N) - B(N - 1) and B the binding energy of the nucleus with N neutrons. The factor depending on the number parity π^N is chosen so that the OES centered on even and odd neutron numbers N will both be positive for normal attractive pairing. It has been pointed out that only in the absence of pairing correlations, $\Delta^{(3)}$ becomes measure of a gap in the single-particle spectrum.

E. Inferences

Is the decrease in gap shown in Fig.7 for Z<14 solely due to the fact that below Z = 14, the size of the gap contain information about additional binding energy due to

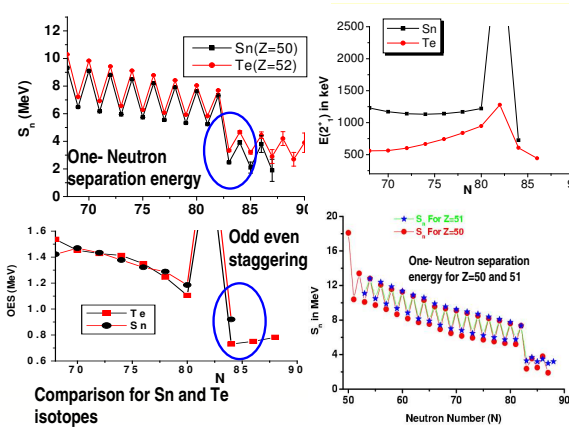

FIG. 9: Correlation of S_n, OES and E(2_1^+) for Sn and Te isotopes.

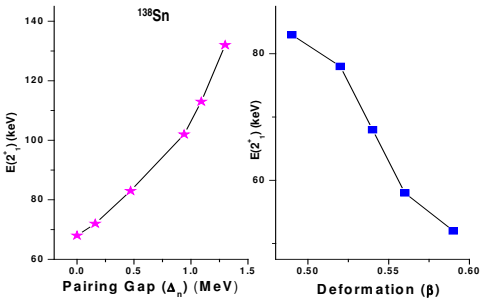

FIG. 10: Evolution of self-consistently calculated E(2_1^+) a functions of deformation and pairing gaps.

quadrupole correlations? Can we not infer that pairing strength is also reduced at those neutron numbers? OES plots also suggest it. The Fig.8 shows the correlations between one neutron separation energies (S_n), OES and E(2_1^+) energies for Ne, Mg, Si and S isotopes. The Ne and Mg isotopes at N=20 show sudden decrease in S_n and the E(2_1^+) energies also show a sudden drop indicating washing away of N=20 shell gap. Similar correlation can be found in other neutron rich domains also. For a demonstration in Fig.9, the correlations for Sn and Te isotopes are shown. The even Sn isotopes have nearly constant E(2_1^+) ($\simeq$ 1200 keV) values for A=102-130. But suddenly for N=84, for ^{134}Sn, the E(2_1^+) value decreases to 726 keV. This can be correlated to the decrease in pairing strength manifested through the reduction in neutron separation energies (S_n), OES and E(2_1^+) energies. We have already discussed that a unique feature is observed in neutron rich isotopes in Ref. [20]. The isotopes of $^{32}Mg_{20}$ has N/Z = 1.67 and $^{30}Ne_{20}$ has N/Z = 2.0. ^{134}Sn is also a neutron rich isotope of Sn having N/Z ratio 1.68. $^{136,138}Te$ isotopes have N/Z =1.62,1.65, respectively. All these isotopes show a sudden depression in 2_1^+. Such large N/Z ratios in many cases have shown new exotic phenomena in nuclear structure. Usually B(E2, $0^+_{g.s.} \rightarrow 2_1^+$) has been found to vary inversely as E(2_1^+) values. But for large N/Z ratios domain this is found to be violated. For Mg isotopes, in ^{24}Mg : E(2_1^+) =1.369 MeV; and B(E2, $0^+_{g.s.} \rightarrow 2_1^+$)=0.0432 (11)$e^2b^2$ $\simeq$21 W.u; but for ^{32}Mg:E(2_1^+)=0.886 MeV; B(E2, $0^+_{g.s.} \rightarrow 2_1^+$)=0.039 (7) e^2b^2 $\simeq$13 W.u. Again for ^{134}Te : E(2_1^+)=1.279 MeV and B(E2, $0^+_{g.s.} \rightarrow 2_1^+$)=0.0960 (120) e^2b^2 $\simeq$4.7 W.u. 136Te: E(2_1^+)=0.606 MeV; B(E2, $0^+_{g.s.} \rightarrow 2_1^+$) =0.1030(150) e^2b^2 $\simeq$5 W.u. So the unusual decrease in E(2_1^+) in ^{32}Mg and ^{136}Te considered to be indications of enhanced collectivity does not show expected degree of

increase in the B(E2, $0^+_{g.s.} \rightarrow 2^+_1$) values.

F. Model Calculations

Representative model calculation has been done using pairing plus quadrupole Hamiltonian within cranked Hartree Fock formalism. It shows (Fig.10) that depressed E(2^+_1) values can result either from reduction of pairing or increase of deformation, keeping all other parameters constant. For reduction of E(2^+_1) due to weakening of pairing, substantial increase of B(E2) value or deformation, β_2 is not observed .

6. Summary

The intruder orbitals from the fp shell play an important role in the structure of nuclei around the line of stability in the upper sd shell both for the negative as well as high spin positive parity states. One of the reasons for the need to decrease or increase of $1d_{3/2}1f_{7/2}$ gap has been found to be directly correlated to the choice of input single particle energy set. This once again shows that the issues relevant for exotic nuclei in the island of inversion should be investigated keeping in mind the observation in nuclei on the stability. The sudden erosion of shell gaps at N=20 for Mg, Ne isotopes may have some correlation with the observed decrease in the odd even mass staggering for these isotopes at these mass numbers. How far the depression of E(2^+_1) energies for ^{32}Mg, ^{30}Ne or ^{134}Sn and $^{136,138}Te$ result from onset of collectivity and/or decrease in the pairing forces need a detail investigation.

Acknowledgments

The experimental part of this work has been done in collaboration with the students and Post-doctoral fellows working in my group and my INGA collaborators. The theoretical part has been done in collaboration with Prof. S. Sarkar, BESU.

References

[1] Ritesh Kshetri *et al.*. Nucl. Phys. A **781**, 277 (2007) and references therein.

[2] Indrani Ray *et al.*, Phys. Rev. C **76**, 034315 (2007).

[3] M. Ionescu-Bujor *et al.* , Phys. Rev. C **80**, 034314 (2009).

[4] C. E. Svensson *et al.*, Phys. Rev. Lett. **85**, 2693 (2000); C. E. Svensson *et al.*, Phys. Rev. C **63**, 061301(R) (2001).

[5] E. Ideguchi *et al.*, Phys. Rev. Lett. **87**, 222501 (2001).

[6] M. Saha Sarkar *et al.*, Nucl. Instr. and Meth. A **491**, 113 (2002).

[7] S. Muralithar *et al.*, Nucl. Instr. and Meth. A **622**, 281 (2010).

[8] Sudatta Ray *et al.*,Proc. DAE-BRNS Symp. Nucl. Phys. (India) **53** (2008) 353.

[9] Rajesh Kumar *et al.*, Proc. DAE-BRNS Symp. Nucl. Phys. **52 B**, 647 (2007); S. Venkataramanan *et al.*, Ibid., **45 B**, 424 (2002); E.T. Subramaniam *et al.*, Rev. Sci. Instr. **77**, 096102 (2006).

[10] Sudatta Ray *et al.*,Proc. DAE-BRNS International Symp. Nucl. Phys. (India), **54** (2009) 56.

[11] R. Bhowmik *et al.*, Proc. DAE-BRNS Symp. Nucl. Phys. **44 B**, 422 (2001).

[12] K. S. Krane and R. M. Steffen, Phys. Rev. C **2**, 724 (1970).

[13] R. Palit *et al.*, Pramana **54**, 347 (2000).

[14] J.C. Wells, N.R. Johnson, Report ORNL-6689, 1991, p 44.

[15] F. Della Vedova *et al.*, Phys. Rev. C **75**, 034317 (2007); J. Ekman *et al.*, Phys. Rev. Lett. **92**, 132502 (2004) and references therein.

[16] T. A. Hinners *et al.*, Phys. Rev. C **77**, 034305 (2008).

[17] O. Sorlin, M. G. Porquet, Prog. Part. and Nucl. Phys. **61**, 602 (2008).

[18] W. Warburton, J.A. Becker, B.A. Brown, Phys. Rev. C **41**, 1147 (1990).

[19] W. Satula, J. Dobaczewski, W. Nazarewicz, Phys. Rev. Lett. **81**, 3599 (1998); W.A. Friedman and G.F. Bertsch, Eur. Phys. J. A **41**, 109 (2009).

[20] S. Sarkar, M. Saha Sarkar, Phys. Rev. C **78**, 024308 (2008).